

# A Mathematical Model of Ebola Virus Disease: Using Sensitivity Analysis to Determine Effective Intervention Targets

**Danny Salem**

Department of Biology  
The University of Ottawa,  
Ottawa ON K1N 6N5 Canada  
dsale017@uottawa.ca

**Robert Smith?**

Department of Mathematics and Faculty of  
Medicine  
The University of Ottawa,  
Ottawa ON K1N 6N5 Canada  
rsmith43@uottawa.ca

## ABSTRACT

Mathematical models provide a useful framework to investigate real-world problems. They can be used in the context of disease dynamics to study how a disease will spread and how we can stop or prevent an outbreak. In December of 2013, an outbreak of Ebola began in the West African country of Guinea and later spread to Sierra Leone and Liberia. Health Organisations like the US Centers for Disease Control and the World Health Organization were tasked with providing aid to end the outbreak. We create an SEIR compartmental model of Ebola with a fifth compartment for the infectious deceased to model the dynamics of an Ebola outbreak in a village of a thousand people. We analyse the disease-free equilibrium of the model and formulate an equation for the eradication threshold  $R_0$ . Sensitivity analyses points us in the direction of the transmission probability and the contact rate with infectious individuals as targets for intervention. We model the effect that vaccination and quarantine, together and separately, have on the outcome of the Ebola epidemic. We find that quarantine is a very effective intervention, but when combined with vaccination it can theoretically lead to eradication of the disease.

## Author Keywords

Ebola; mathematical model; Latin hypercube sampling; partial rank correlation coefficients

## INTRODUCTION

In December of 2013, an outbreak of Ebola Virus Disease began in the West African country of Guinea and later spread to neighbouring countries Liberia and Sierra Leone. By November 4th, 2014, the outbreak had reached 13,268 cases, 27 of which had spread to neighbouring countries and overseas in Senegal, Nigeria, Mali, Spain and the US [5].

Ebola Virus Disease (known simply as Ebola) is caused by the epizootic Ebola Virus, which is thought to be found in mammals of the family Pteropodidae (aka fruit bats) [17].

Transmission of the virus can occur from bats to other mammals, usually chimpanzees, gorillas and baboons [2]. Infection of humans can occur through contact with bodily fluids of these animals. Transmission from infected to susceptible humans occurs through direct contact with the saliva, mucus, vomit, faeces, sweat, tears, breast milk, urine and semen of an infected individual. Since direct contact of bodily fluids is necessary, the points of entry of the virus include the nose, mouth, open wounds, eyes, abrasions and cuts [14]. Symptoms include fever, sore throat, muscle pains and headaches, followed by vomiting, diarrhoea, rashes and decreased function of the kidney and liver, then internal and external bleeding. The risk of death from the disease is around 50%, increasing as the disease progresses to the bleeding stage [1]. This is also the stage at which infected individuals become infectious. Unprotected contact with infected corpses at Guinean burial rituals are suspected to have been the cause of over 60% of cases in Guinea [8], which is potentially a self-perpetuating problem.

Information obtained from mathematical models can help determine the necessary response to an outbreak [19]. Most models, including recent ones used to model the current outbreak, use the basic reproduction number or similar threshold ( $R_0$ ) of a virus to quantitatively describe the trend of an epidemic. The reproduction number is the measure of the transmission potential of a virus or, in other words, the average number of susceptible people that one infected individual will infect. The interpretation of the  $R_0$  value is that if it is greater than 1, then more people are getting infected over time and the epidemic is spreading, while if the value is less than 1, the epidemic is dying off, since fewer people are getting infected [15]. In this sense, there is a threshold when  $R_0$  is equal to 1; at this point, any perturbations will either lead to the end or continuation of the epidemic. We decided to use a compartmental model to describe the Ebola outbreak in West Africa. Using this model, we were able to determine an equation for  $R_0$  and investigate the effect of different interventions on  $R_0$ .

A handful of compartmental models have already addressed the recent Ebola outbreak. Rivers *et al.* [23] investigated the efficiency of increased contact tracing, improved infection-control practices and a hypothetical pharmaceutical interven-

tion to improve survival of hospitalised patients aimed at reducing the reproduction number of the Ebola virus. They showed that perfect contact tracing could reduce  $R_0$  from 2.22 to 1.89, while additionally reducing hospitalisation rates by 75% would further reduce  $R_0$  to 1.72. Chowell *et al.* [9] used an SEIR model to determine  $R_0$ , the final size of the epidemic and performed a sensitivity analysis, showing that education and contact tracing with quarantine would reduce the epidemic by a factor of 2. Fisman *et al.* [13] used a two-parameter model to examine epidemic growth and control. They evaluated the growth patterns and determined the degree to which the epidemic was being controlled, finding only weak control in West Africa as of the end of August 2014 and essentially no control in Liberia. Webb and Browne [25] developed an age-structured model, tracking disease age through initial incubation, followed by an infectious phase with variable transmission infectiousness. They showed that successive stages of hospitalisation have resulted in a mitigation of the epidemic. Browne *et al.* [7] developed an SEIR model to examine the effects of contact tracing and determine  $R_0$ . They showed that, if contact tracing was perfect, then the critical proportion of contacts that need to be traced could be derived. Do and Lee [12] developed an SLIRD model to determine the mathematical dynamics of the disease. Their model had a single equilibrium point, which they showed would be stable if safe burial practices without traditional rituals were followed and  $R_0 < 1$ .

Here we propose a compartmental model consisting of five groups of individuals: susceptible ( $S$ ), non-symptomatic infected ( $E$ ), infectious living ( $I$ ), infectious deceased ( $D_I$ ) and recovered ( $R$ ). We include the dead as an actively infectious compartment in our model. We have previously performed such modelling in other contexts [20]; while Ebola is more serious and the dead do not move about, there are nevertheless some similarities in the model construction.

## THE MODEL

We used standard incidence to represent contact between susceptible ( $S$ ) and infected ( $I, D_I$ ) individuals since contact between susceptible and infected individuals is not well-mixed, occurring disproportionately more at burial rituals [8]. We modelled a representative West African village of 1000 individuals, on the basis that contact rates would be close to uniform in a small and relatively isolated population. The infected deceased ( $D_I$ ) are included in the denominator for the rate of infection since they are interacting with susceptible individuals, making them an active part of the population ( $N$ ). We include permanent immunity in the model but assume that no susceptible individuals have pre-existing immunity; this has been shown to occur [11], but we choose not to incorporate it, since the frequency of mutation is currently unknown. We make the assumption that non-symptomatic infected individuals ( $E$ ) do not become infectious dead if they die at the background death rate.

The model is described by the following five differential equations:

$$S' = \Lambda - \frac{\beta c_I SI}{S + E + I + R + D_I} - \frac{\beta c_d SD_I}{S + E + I + R + D_I} - \mu S$$

New susceptible ( $S$ ) individuals enter the population at a constant birth/immigration rate ( $\Lambda$ ). Susceptible individuals may die and leave the population at the background death rate ( $\mu S$ ), or they may be infected and enter the non-symptomatic infected compartment ( $E$ ) at the infection rate that is represented by the two fractions.

$$E' = \frac{\beta c_I SI}{S + E + I + R + D_I} + \frac{\beta c_d SD_I}{S + E + I + R + D_I} - (\omega + \mu)E$$

Newly infected individuals enter the compartment at the same rate susceptible people get infected. Non-symptomatic infected individuals become infectious and symptomatic, thereby leaving the compartment and joining the symptomatic infected compartment at rate  $\omega E$ . Non-symptomatic infected individuals die at the background death rate ( $\mu E$ ).

$$I' = \omega E - (\alpha + \gamma)I$$

Infected individuals become symptomatic at rate ( $\omega E$ ). Symptomatic infectious individuals may leave the compartment via disease death (at rate  $\alpha I$ ) or through recovery (at rate  $\gamma I$ ) joining the recovered ( $R$ ) compartment, where they are immune to infection.

$$R' = \gamma I - \mu R$$

The number of recovered individuals increases due to recovery (at rate  $\gamma I$ ), and it decreases due to background death (at rate  $\mu R$ ).

$$D_I' = \alpha I - \theta D_I$$

The number of infected deceased increases due to death from the disease (at rate  $\alpha I$ ), and it decreases as dead bodies lose their infectivity (at rate  $\theta D_I$ ). The model is shown in Figure 1.

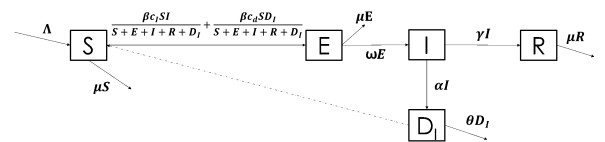


**Figure 1.** Model Flowchart. The movement of individuals through the compartments via infection, recovery and death. At birth, individuals are susceptible ( $S$ ). They may die from unrelated causes and exit the system, or they may be infected either by an infectious individual or corpse and become non-symptomatic infected ( $E$ ). Non-symptomatic infected individuals become infectious ( $I$ ), or they can die from an unrelated cause and exit the system. Infectious individuals can recover ( $R$ ) from the disease or they may die from the disease and become an infectious dead body ( $D_I$ ). Recovered individuals can no longer be infected; they die at the background death rate. Infectious dead bodies stop being infectious after safe burial or after the live virus is no longer in the corpse.

These five equations represent the rate of change over time of five different categories of individuals within a village undergoing an Ebola epidemic. The infected deceased compartment ( $D_I$ ) represents the dead bodies of previously infected individuals who are still capable of infecting susceptible individuals. This infection of susceptible individuals by infected dead bodies is represented in Figure 1 by the dotted line connecting the Susceptible ( $S$ ) and the Infected Deceased ( $D_I$ ) compartments. People who are infected are not infectious until they are symptomatic [1]; as a result, once individuals from the susceptible group are infected, they join the non-symptomatic infected group before joining the infectious group.

## ANALYSIS

We are interested in the stability of the disease-free equilibrium (DFE), which is given by the expression

$$(S^0, E^0, I^0, R^0, D_I^0) = \left( \frac{\Lambda}{\mu}, 0, 0, 0, 0 \right).$$

The disease-free equilibrium is the point in the epidemic where there are no infected ( $I, E$ ), recovered ( $R$ ) or infected deceased ( $D_I$ ) individuals in the system; in other words, the epidemic is not occurring. To analyse the dynamics of the system near the equilibrium, we calculated the Jacobian matrix and evaluated it at the DFE:

$$J_{DFE} = \begin{bmatrix} -\mu & 0 & -\beta c_I & 0 & -\beta c_D \\ 0 & -\omega - \mu & \beta c_I - \gamma & 0 & \beta c_D \\ 0 & \omega & -\alpha - \gamma & 0 & 0 \\ 0 & 0 & \gamma & -\mu & 0 \\ 0 & 0 & \alpha & 0 & -\theta \end{bmatrix}.$$

Two of the eigenvalues of this matrix are  $\lambda = -\mu, -\mu$ , which are both negative (since all parameters are positive). The remaining three eigenvalues of the Jacobian matrix are given by the characteristic equation

$$\lambda^3 + (\alpha + \gamma + \theta + \omega + \mu)\lambda^2 + (\omega\alpha + \omega\gamma + \omega\theta + \mu\alpha + \mu\gamma + \mu\theta + \alpha\theta + \gamma\theta + \beta c_I\omega)\lambda + \theta(\omega\alpha + \omega\gamma + \mu\alpha + \mu\gamma) - \beta c_I\omega\theta - \beta c_D\omega\alpha = 0.$$

If we represent the equation by

$$a_3\lambda^3 + a_2\lambda^2 + a_1\lambda + a_0 = 0,$$

then, according to the Routh–Hurwitz Criterion, the following two criteria are necessary for the equilibrium to be locally asymptotically stable:

1.  $a_n > 0$  ( $n = 0, 1, 2, 3$ )
2.  $a_1 a_2 > a_3 a_0$ .

First, we look at the second criterion:

$$(\alpha + \gamma + \theta + \omega + \mu)(\omega\alpha + \omega\gamma + \omega\theta + \mu\alpha + \mu\gamma + \mu\theta + \alpha\theta + \gamma\theta + \beta c_I\omega) > \theta(\omega\alpha + \omega\gamma + \mu\alpha + \mu\gamma) - \beta c_I\omega\theta - \beta c_D\omega\alpha.$$

The term  $\theta(\omega\alpha + \omega\gamma + \mu\alpha + \mu\gamma)$  appears on both sides of the inequality, which means it can be subtracted from both sides. Since every parameter is positive, we are left with a positive

term on the left-hand side and a negative term on right-hand side, so the second criterion holds.

Next we look at the  $a_n > 0$  criteria. The  $a_3, a_2, a_1$  terms are all positive. So the only condition to be met is:

$$(\omega\alpha\theta + \omega\gamma\theta + \mu\alpha\theta + \mu\gamma\theta) - \beta c_I\omega\theta - \beta c_D\omega\alpha > 0.$$

If this condition is not met, then the DFE is unstable and the epidemic will spread. If the condition is met, then the DFE is stable and the epidemic will end. This gives us a threshold condition [15] from which we can derive an eradication threshold:

$$R_0 = \frac{(\beta c_I\omega\theta + \beta c_D\omega\alpha)}{\theta(\omega\alpha + \omega\gamma + \mu\alpha + \mu\gamma)}.$$

It should be noted that  $R_0$ -like thresholds calculated from differential equation models are not necessarily the reproduction number; however, they share a stability threshold [18]. Specifically, if  $R_0 < 1$ , then the DFE is (locally) stable, whereas if  $R_0 > 1$ , the DFE is unstable. However, such results do not establish global stability or rule out the presence of a backward bifurcation. The latter can sometimes be observed numerically, although our simulations did not discern one. Nevertheless, such thresholds can be useful for understanding eradication.

To investigate the relationship between the contact rates and the transmission probability, we set  $R_0$  to 1 and isolate  $\beta$ :

$$\beta = \frac{\theta(\omega\alpha + \omega\gamma + \mu\alpha + \mu\gamma)}{(c_I\omega\theta + c_D\omega\alpha)}.$$

We assigned the sample values found in Table 1 to all the parameters except the contact rates and plotted three variables of interest,  $\beta$ ,  $c_I$  and  $c_D$  (Figure 2). The resulting surface represents the eradication threshold. From the lopsided slope of the surface, we see that  $R_0$  is influenced less by  $c_D$  than  $c_I$ . It follows that human-to-human contact is a greater driver of the epidemic than that of the infectious dead.

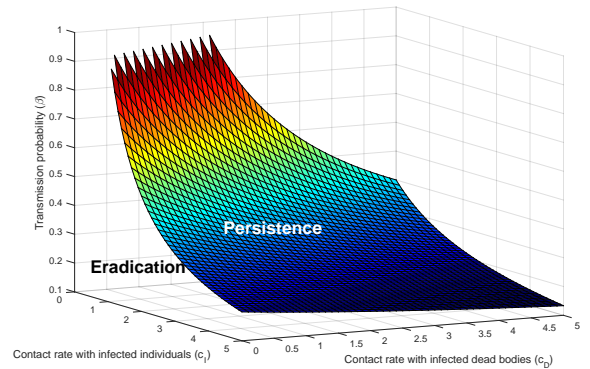


**Figure 2.** Mesh plot of transmission probability ( $\beta$ ) as a function of the contact rates ( $c_D, c_I$ ) when  $R_0=1$ , with other parameters set to their median values from Table 1. The surface of this function is the threshold of the epidemic. The disease will persist if parameters are above the surface, while it will be eradicated if they are below it.

Next, we calculated the partial derivatives of  $R_0$  with respect to all eight parameters. Positive partial derivatives indicate

Parameter	Description	Range	Sample Value	Units	Reference
$\alpha$	disease death rate	0.5–1	0.5	weeks <sup>-1</sup>	[24]
$\gamma$	recovery rate	0.5–1	0.5	weeks <sup>-1</sup>	[16]
$\mu$	background death rate	0–0.001	1/50	years <sup>-1</sup>	[10]
$\Lambda$	birth rate	0–1	1000 $\mu$	people years <sup>-1</sup>	[10]
$\theta$	safe burial rate	0.33–7	1	weeks <sup>-1</sup>	[22]
$c_I$	contact rate with infectious individuals	0–5	variable	people weeks <sup>-1</sup>	-
$c_D$	contact rate with infectious dead bodies	0–5	variable	people weeks <sup>-1</sup>	-
$\beta$	transmission probability	0–1	0.75	-	assumed
$\omega$	rate at which infected individuals becoming infectious	0.33–3	1	weeks <sup>-1</sup>	[1]

**Table 1.** Parameter values. Each parameter is described, and the range and sample values found in literature are listed. The inverse of the rate parameters represent the average duration of time that the process takes.

that an increase in that parameter will increase  $R_0$ , whereas negative partial derivatives indicate that an increase in that parameter will decrease  $R_0$ .

$$\frac{\partial R_0}{\partial \beta} = \frac{c_I \omega \theta + c_D \omega \alpha}{\theta(\omega \alpha + \omega \gamma + \mu \alpha + \mu \gamma)} > 0$$

(transmission probability)

$$\frac{\partial R_0}{\partial c_I} = \frac{\beta \omega}{\omega \alpha + \omega \gamma + \mu \alpha + \mu \gamma} > 0$$

(contact rate with infected)

$$\frac{\partial R_0}{\partial c_D} = \frac{\beta \omega \alpha}{\theta(\omega \alpha + \omega \gamma + \mu \alpha + \mu \gamma)} > 0$$

(contact with the dead)

$$\frac{\partial R_0}{\partial \omega} = \frac{(\beta c_I \theta + \beta c_D \alpha)(\theta \mu \alpha + \theta \mu \gamma)}{(\theta \omega \alpha + \theta \omega \gamma + \theta \mu \alpha + \theta \mu \gamma)^2} > 0$$

(rate of becoming infectious)

$$\frac{\partial R_0}{\partial \mu} = \frac{-(\theta \alpha + \theta \gamma)(\beta c_I \theta \omega + \beta c_D \alpha \omega)}{(\theta \omega \alpha + \theta \omega \gamma + \theta \mu \alpha + \theta \mu \gamma)^2} < 0$$

(death rate)

$$\frac{\partial R_0}{\partial \gamma} = \frac{-(\theta \omega + \theta \mu)(\beta c_I \theta \omega + \beta c_D \alpha \omega)}{(\theta \omega \alpha + \theta \omega \gamma + \theta \mu \alpha + \theta \mu \gamma)^2} < 0$$

(recovery rate)

$$\frac{\partial R_0}{\partial \theta} = \frac{-(\omega \alpha + \omega \gamma + \mu \alpha + \mu \gamma)(\beta c_D \alpha \omega)}{(\theta \omega \alpha + \theta \omega \gamma + \theta \mu \alpha + \theta \mu \gamma)^2} < 0$$

(safe burial rate)

$$\frac{\partial R_0}{\partial \alpha} = \frac{\beta c_D \omega^2 \theta \gamma + \beta c_D \omega \theta \mu \gamma - (\beta c_I \omega^2 \theta^2 + \beta c_I \omega \theta^2 \mu)}{(\theta \omega \alpha + \theta \omega \gamma + \theta \mu \alpha + \theta \mu \gamma)^2}$$

(disease death rate)

For the latter, we have

$$\frac{\partial R_0}{\partial \alpha} > 0 \quad \text{if} \quad \frac{c_D}{\theta} > \frac{c_I}{\gamma} \quad \text{and} \quad \frac{\partial R_0}{\partial \alpha} < 0 \quad \text{if} \quad \frac{c_D}{\theta} < \frac{c_I}{\gamma}$$

The first seven partial derivatives here match the sign of the Partial Rank Correlation Coefficients (PRCCs) calculated for their respective parameters (Figure 3). The PRCC calculated for the disease death rate ( $\alpha$ ) is negative. We determined that the partial derivative would only be negative if  $\frac{c_D}{\theta} < \frac{c_I}{\gamma}$ ; that is, if the ratio of contact with the dead to safe burial is lower than the ratio of contact with the infected to the recovery rate. This implies that, if dead bodies are sufficiently infectious, then a higher death rate will increase the overall risk. The equality  $\frac{c_D}{\theta} = \frac{c_I}{\gamma}$  represents a critical case, the threshold beyond which the epidemic will spiral out of control.

In our case, since the ranges for the contact rates used in our Latin Hypercube Sampling were the same and the range for  $\theta$  is higher than  $\gamma$  (Table 1), we will usually have  $\frac{c_D}{\theta} < \frac{c_I}{\gamma}$ . It follows that an increased death rate from Ebola will lower the overall risk.

## NUMERICAL SIMULATIONS

We performed sensitivity analyses on all the parameters using partial rank correlation coefficient (PRCC) analysis. PRCCs measure the relative degree of sensitivity of the outcome variable to each parameter, regardless of whether the parameter has a positive or negative influence on the outcome variable. We use PRCCs to rank the influence of the parameters in our model on  $R_0$ . This is done computationally by sampling parameters from a uniformly distributed range using Latin Hypercube Sampling (LHS), a statistical sampling method that evaluates sensitivity of an outcome variable to all input variables. The parameters were sampled 1000 times for 1000 runs.

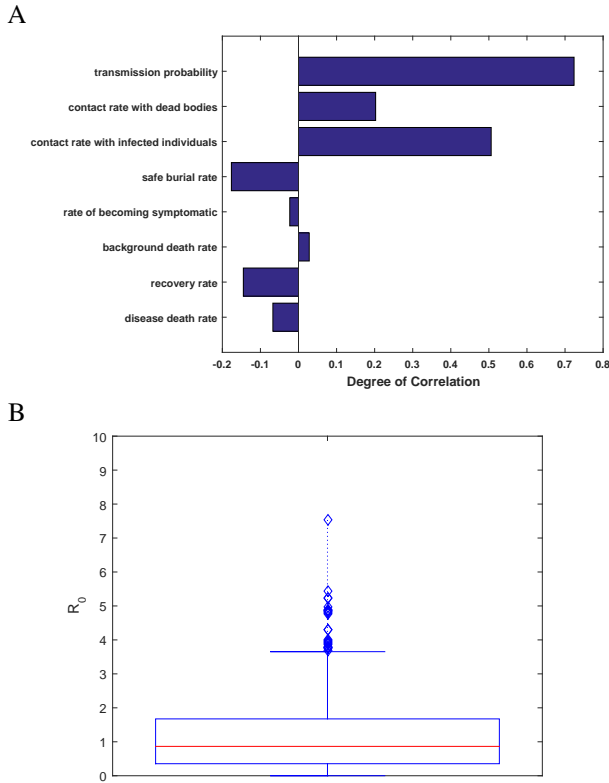


**Figure 3.** A. Partial Rank Correlation Coefficient sensitivity analysis of parameters. Sensitivity analysis of  $R_0$  with respect to all the parameters. B. Box plot of all 1000  $R_0$  values. Latin Hypercube Sampling (LHS) was used to sample parameters. The LHS ranges are given in Table 5.1. The horizontal red line indicates the median of all 1000 of the  $R_0$  values. 54% of the values lie underneath  $R_0 = 1$ .

Inclusion of interventions in the model was achieved by modifying the ranges for the parameters targeted by the intervention. For example, to increase the number of safe burial teams, we increased the rates of safe burial ( $\theta$ ) and reran our PRCC analyses. To examine quarantine and isolation, we decreased the range of the contact rate with infected individuals ( $c_I$ ). We used a script to check each value of  $R_0$  to determine if it was less than 1. All numerical simulations were completed using MATLAB.

### SENSITIVITY ANALYSIS

Figure 3A shows the PRCCs of the eight parameters found in our equation for  $R_0$ . We find that, at the disease-free equilibrium,  $R_0$  is most influenced by the transmission probability, the amount of contact with the dead and the contact rates between infected individuals and susceptible individuals. All three parameters will increase  $R_0$  when they are increased, since the PRCCs point to the right. While increasing the safe burial rate will have a reductive effect on the epidemic (since its PRCC points to the left), this effect is swamped by the others. Figure 3B illustrates all 1000  $R_0$  values calculated from the sampled parameter values in a boxplot. The horizontal red line indicates the median  $R_0$  value and the whiskers are found at the first and third quartiles. We find that 54% of the  $R_0$  values lie underneath the threshold  $R_0 = 1$ .

Figure 4 shows the changes observed in  $R_0$  as each of the four most influential parameters change, compared to the eradication threshold (horizontal line) in the absence of interventions. A decrease in  $R_0$  is associated with an increase of the safe burial rate and a decrease in the transmission probability or the contact rates. The most defined trend is found in the transmission probability.

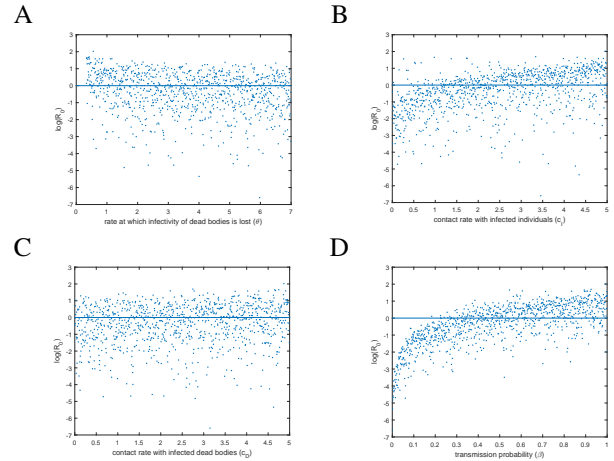


**Figure 4.** LHS output for  $R_0$  as a factor of the four most influential parameters: (A) the safe burial rate  $\theta$ , (B) the contact rate with infectious individuals  $c_I$ , (C) the contact rate with infectious dead bodies  $c_D$  and (D) the transmission probability  $\beta$ . Values for all nine parameters were sampled 1000 times. The horizontal line indicated the threshold  $R_0 = 1$ .

### INTERVENTIONS

To investigate the effectiveness of an intervention targeting the safe burial rate, we adjusted the range that we sampled from for our sensitivity analyses. The sampled range was changed from 0.33–7 weeks<sup>-1</sup> to 2–7 weeks<sup>-1</sup>. (Note that the duration of risk of a dead body is inversely proportional to these numbers.) Figure 5A illustrates the revised sensitivity of all eight parameter values subject to the adjusted range for the safe burial rate. We find that, with an improved safe burial task force, the contact rate with dead bodies is no longer as influential on  $R_0$ . The boxplot in Figure 5B shows that 60% of the  $R_0$  values lie underneath the threshold  $R_0 = 1$ , a substantial improvement over the previous analysis.

Next, we examined the effect of improved quarantine and isolation techniques by reducing the range of  $c_I$  from 0–5 people/week to 0–1 people/week. All other parameters were at their original sample values. Figure 5C shows that the contact rate with infected individuals has been reduced, while the safe burial rate is now a significant factor. It follows that, if contact between susceptible and infected individuals is reduced, then efforts must be made to ensure safe burial practices are maintained, so that the epidemic is not sustained by infection from the dead. The boxplot in Figure 5D shows that 90% of all  $R_0$  values are now found below the threshold  $R_0 = 1$ .

Finally, Figure 6 illustrates the LHS output of  $R_0$  as a function of the transmission probability, using all 1000 sampled values. (Each dot represents a simulation.) The parameter ranges used for this plot are as in Figure 5C and 5D, illustrating the effect that quarantine and isolation intervention would

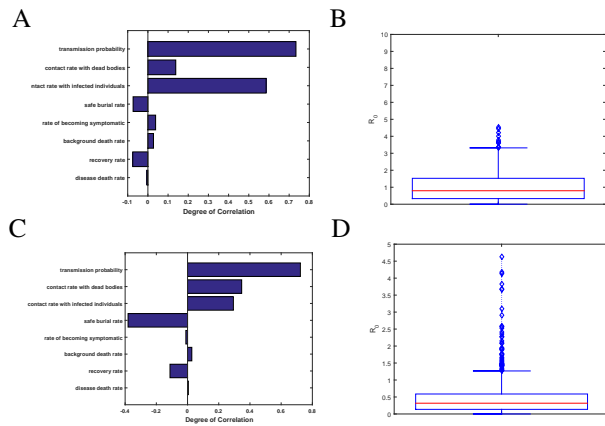


**Figure 5.** A. Partial Rank Correlation Coefficients sensitivity analysis of parameters with modified safe burial rate. The safe burial rate  $\theta$  is modified, shrinking the range from 0.33–7 to 2–7 weeks<sup>-1</sup>, which indicates the longest a dead body remains infectious is three and a half days. B. Box plot of all 1000  $R_0$  values with modified safe burial rate. 60% of the values lie underneath  $R_0 = 1$ . C. Partial Rank Correlation Coefficient sensitivity analysis of parameters with modified  $c_I$ . A decreased contact rate with infected individuals is introduced by modifying the range of  $c_I$  used in LHS from 0–5 to 0–1, which indicates that on average the highest number of infectious individuals a susceptible person can come in contact with is 1 per week. D. Box plot of all 1000  $R_0$  values with modified  $c_I$ . 90.5% of the values lie underneath  $R_0 = 1$ .

have on  $R_0$ . We see that, as calculated earlier, 90% of the  $R_0$  values are below 1. Without interventions, 98% of the values of  $R_0$  are less than 1 when the transmission probability is less than 0.3. With quarantine, 98% of all  $R_0$  values are less than 1 when the transmission probability is less than 0.5.

## DISCUSSION

According to our results, the parameters with the greatest effect on the Ebola epidemic are the transmission probability ( $\beta$ ), the safe burial rate ( $\theta$ ) and the two contact rates ( $c_I$ ,  $c_D$ ). However, the contact rate between infected and susceptible individuals has considerably more influence on the outcome. This is likely because infected individuals lose their infectivity slower than infected dead bodies do. Infectious dead bodies remain infectious for up to a week after death [22], and they can easily be rendered safe through careful burial. The transmission probability is the most influential parameter in the  $R_0$  equation. Although we have separated the contact rates from the transmissibility of the virus, our results indicate that any efforts to reduce this transmission, such as a vaccine or treatment, would have a significant effect on reducing the overall epidemic.

There are several interventions that have already been used to reduce the spread of Ebola. Quarantine of individuals found through aggressive contact tracing [6] and isolation of infected individuals while they are treated have been effective methods to reduce the contact rates with infected individuals [4]. To deal with the problem of infected dead bodies on the street and unsafe burial rituals, the US Centers for Disease Control (CDC) has employed safe burial teams, which are tasked with safely burying corpses [21]. This increases the rate at which dead bodies lose their infectivity; as a re-

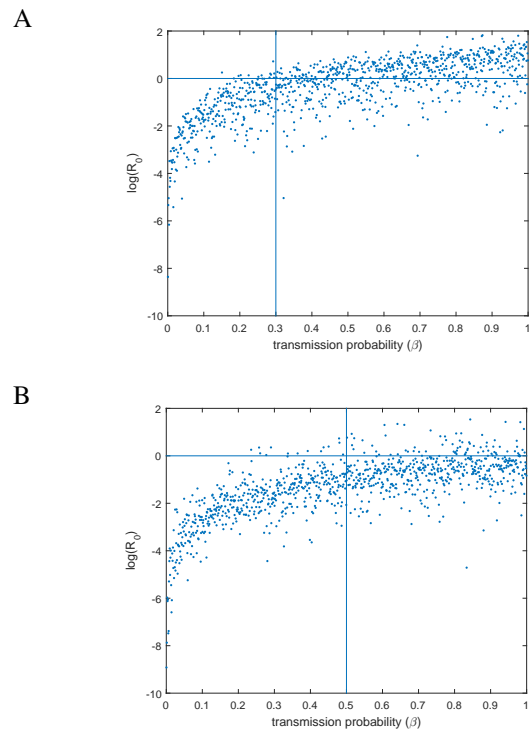


**Figure 6.** LHS output for  $R_0$  as a factor of transmission probability ( $\beta$ ) with modified  $c_I$ . A. When  $\beta < 0.3$ , 98% of the values lie underneath  $R_0 = 1$ . B. Applying quarantine decreased the contact rate with infected individuals by modifying the range of  $c_I$  used in LHS from 0–5 to 0–1, which indicates that on average the highest amount of infectious individuals a susceptible person can come in contact with is 1 per week. In this case, 98% of  $R_0$  values were below 1 when  $\beta < 0.5$ .

sult, there is less contact between susceptible individuals and infected dead bodies.

The employment of safe burial teams was a significant factor during the recent Ebola outbreak. Effectively, this increases the safe burial rate ( $\theta$ ). We investigate the effectiveness of this intervention by using a modified range for the safe burial rate ( $\theta$ ) and observing the changes in our LHS output (Figure 5). We found that the influence of the rate of contact with infected dead bodies was consequently reduced (Figure 5A). However, the overall effectiveness of increasing the safe burial rate is limited, only increasing the number of simulation values below the eradication threshold from 54% (Figure 3) to 60% (Figure 5). It follows that efforts to reduce contact need to be diversified, even if dead bodies are being dealt with in a timely manner.

There have been recent trials for an Ebola vaccine, some of which have been promising [3]. A perfect vaccine would reduce the susceptible pool; however, even an imperfect vaccine would likely lower the transmissibility. In practice, interventions should be instituted in tandem. Combining quarantine and vaccination (by reducing both the contact rate and the transmissibility) will lead to disease eradication. As shown in Figure 6, decreasing the transmissibility below  $\beta = 0.5$ , when the quarantine is applied, would result in 98% of the cases having an  $R_0$  value below 1, which would ultimately

lead to the eradication of the epidemic. Figure 2 shows that, with a low transmission probability, eradication can still occur even with high contact rates.

Our model has several limitations, which should be acknowledged. We assumed constant birth/immigration and background death rates, which may not hold as populations move about, as they may in response to the disease. We assumed the same transmission probability for the living and dead, which may not be true. We also made the assumption that individuals who die from other reasons could not be infected with Ebola after death, which may have a much larger effect on sustaining the epidemic.

It should be noted that our model bears a high degree of similarity to the work of Do and Lee [12]. It is the nature of an emerging outbreak that multiple models may be developed in parallel during the same research period, which may produce similar constructions. Despite the similarities, there are a number of key differences: their model included both transmission and “infectious death” of latently infected individuals, which ours didn’t. Conversely, we included birth and death rates, as well as the “aging out” of the infectious dead. Furthermore, our focus was on using sensitivity analysis to explore the effect of parameter variation, in order to determine effective intervention targets.

Future work will model the effects of a potential vaccine. With initial trials yielding positive results [3], it is very likely that, in the coming years, there will be an approved vaccine available for use in at-risk countries. Determining the portion of the population required for there to be effective herd immunity and determining the right age to vaccinate people will be investigated. We will also model quarantine explicitly using a separate compartment and account for the role of superspreaders using impulsive differential equations.

During the recent outbreak in West Africa, public-health education programs, quarantine, safe burial initiatives and other interventions were instituted in an attempt to reduce  $R_0$  below 1 and eventually end the epidemic. We have shown that doing so is necessary to ensure the end of an epidemic, since no single intervention was enough to bring all the  $R_0$  values in our model below the threshold on its own. If there is success in the recent trials for the Ebola vaccine, then a public-health program to vaccinate as much of the population as possible is necessary to prevent future outbreaks. However, before such a program is possible, the combination of other interventions will be necessary to end the current outbreak in West Africa and any other outbreaks that occur from now until a time where we have a widely available vaccine.

#### ACKNOWLEDGEMENTS

We thank David Sankoff for technical discussions and are grateful to Jacob Barhak, Young Lee and Ates Hailegiorgis for their thoughtful reviews that improved the manuscript. RS? is supported by an NSERC Discovery Grant. For citation purposes, note that the question mark is part of the author’s name.

#### REFERENCES

1. Ebola virus disease fact sheet. Tech. rep., World Health Organization, April 2015.
2. Acha, P. N., and Szyfres, B. *Zoonoses and Communicable Diseases Common to Man and Animals, 3rd edition*. Pan American Health Organization, 2003.
3. Agnandji, S. T., Huttner, A., Zinser, M. E., Njuguna, P., Dahlke, C., Fernandes, J. F., Yerly, S., Dayer, J.-A., Kraehling, V., Kasonta, R., et al. Phase 1 trials of rVSV Ebola vaccine in Africa and Europe — preliminary report. *New England Journal of Medicine* (2015).
4. Alazard-Dany, N., Terrangle, M. O., and Volchkov, V. Ebola and Marburg viruses: the humans strike back. *M/S: médecine sciences* 22, 4 (2006), 405–410.
5. Aylward, B., et al. Ebola virus disease in West Africa — the first 9 months of the epidemic and forward projections. *N Engl J Med* 371, 16 (2014), 1481–95.
6. Bausch, D. G., Towner, J. S., Dowell, S. F., Kaducu, F., Lukwiya, M., Sanchez, A., Nichol, S. T., Ksiazek, T. G., and Rollin, P. E. Assessment of the risk of Ebola virus transmission from bodily fluids and fomites. *Journal of Infectious Diseases* 196, Supplement 2 (2007), S142–S147.
7. Browne, C., Gulbudak, H., and Webb, G. Modeling contact tracing in outbreaks with application to Ebola. *Journal of Theoretical Biology* 384 (2015), 33–49.
8. Chan, M. Ebola virus disease in West Africa — no early end to the outbreak. *New England Journal of Medicine* 371, 13 (2014), 1183–1185.
9. Chowell, G., Hengartner, N. W., Castillo-Chavez, C., Fenimore, P. W., and Hyman, J. M. The basic reproductive number of Ebola and the effects of public health measures: the cases of Congo and Uganda. *Journal of Theoretical Biology* 229 (2004), 119–126.
10. CIA. CIA World Factbook, Liberia, 2010.
11. Côté, M., Misasi, J., Ren, T., Bruchez, A., Lee, K., Filone, C. M., Hensley, L., Li, Q., Ory, D., Chandran, K., et al. Small molecule inhibitors reveal niemann-pick c1 is essential for Ebola virus infection. *Nature* 477, 7364 (2011), 344–348.
12. Do, T. S., and Lee, Y. S. Modeling the spread of Ebola. *Osong Public Health and Research Perspectives* 7 (2016), 43–48.
13. Fisman, D., Khoo, E., and Tuite, A. Early epidemic dynamics of the West African 2014 Ebola outbreak: Estimates derived with a simple two-parameter model. *PLoS Currents* 6 (2014).
14. Funk, D. J., and Kumar, A. Ebola virus disease: an update for anesthesiologists and intensivists. *Canadian Journal of Anesthesia/Journal canadien d’anesthésie* 62, 1 (2015), 80–91.
15. Heffernan, J. M., Smith, R. J., and Wahl, L. M. Perspectives on the basic reproductive ratio. *Journal of the Royal Society Interface* 2, 4 (2005), 281–293.

16. Hunter, G. W., and Strickland, G. T. *Hunter's tropical medicine and emerging infectious diseases*, vol. 857. WB Saunders company, 2000.
17. Leroy, E. M., Kumulungui, B., Pourrut, X., Rouquet, P., Hassanin, A., Yaba, P., Délicat, A., Paweska, J. T., Gonzalez, J.-P., and Swanepoel, R. Fruit bats as reservoirs of Ebola virus. *Nature* 438, 7068 (2005), 575–576.
18. Li, J., Blakeley, D., and Smith?, R. The failure of  $R_0$ . *Computational and Mathematical Methods in Medicine* 2011 (2011), Article ID 527610.
19. Moghadas, S., et al. Modelling an influenza pandemic: A guide for the perplexed. *Canadian Medical Association Journal* 181, 3-4 (2009), 171–173.
20. Munz, P., Hudea, I., Imad, J., and Smith?, R. When zombies attack!: Mathematical modelling of an outbreak of zombie infection. In *Infectious Disease Modelling Research Progress*, J. M. Tchuente and C. Chiyaka, Eds. Nova Science, 2009, 133–150.
21. Nielsen, C. F., Kidd, S., Sillah, A. R., Davis, E., Mermin, J., and Kilmarx, P. H. Improving burial practices and cemetery management during an Ebola virus disease epidemic — Sierra Leone, 2014. *MMWR. Morbidity and mortality weekly report* 64, 1 (2015), 20–27.
22. Prescott, J., et al. Postmortem stability of Ebola virus. *Emerging Infectious Diseases* 21 (2015).
23. Rivers, C. M., Lofgren, E. T., Marathe, M., Eubank, S., and Lewis, B. L. Modeling the impact of interventions on an epidemic of Ebola in Sierra Leone and Liberia. *PLOS Currents Outbreaks* (2014).
24. Singh, S. K., and Ruzek, D. *Viral hemorrhagic fevers*. CRC Press, 2014.
25. Webb, G., and Browne, C. A model of the Ebola epidemics in West Africa incorporating age of infection. *Journal of Biological Dynamics* 10 (2016), 18–30.